

SUMMARY OF LOCE L2-2/L2-3 ANALYSIS
AND LOFT/ZION PROTOTYPIC STUDY

J. H. Linebarger

DISCLAIMER

This report was prepared as an account of work sponsored by an agency of the United States Government. Neither the United States Government nor any agency thereof, nor any of their employees, makes any warranty, express or implied, or assumes any legal liability or responsibility for the accuracy, completeness, or usefulness of any information, apparatus, product, or process disclosed, or represents that its use would not infringe privately owned rights. Reference herein to any specific commercial product, process, or service by trade name, trademark, manufacturer, or otherwise does not necessarily constitute or imply its endorsement, recommendation, or favoring by the United States Government or any agency thereof. The views and opinions of authors expressed herein do not necessarily state or reflect those of the United States Government or any agency thereof.

DISCLAIMER

Portions of this document may be illegible in electronic image products. Images are produced from the best available original document.

CONTENTS

INTRODUCTION	1
L2-2/L2-3 ANALYSIS	1
LOFT/ZION PROTOTYPIC STUDY	3

FIGURES

1. L2-2/L2-3 cladding temperature comparison	8
2. Cold leg mass flows	9
3. L2-3 cladding temperature versus SPND output	10
4. Cladding deformation	11
5. Fuel cladding temperature comparison	12
6. Fuel cladding temperature comparison	13
7. Broken loop cold leg mass flow comparison	14
8. Intact loop(s) cold leg mass flow comparison	15
9. Comparative cold leg mass flow balance (Intact--Broken) . . .	16
10. Core inlet mass flux ratio from RELAP4/MOD6 calculations . . .	17
11. Core inlet density ratio from RELAP4/MOD6 calculations	18

TABLES

1. Initial Conditions for LOCE L2-2 and LOCE L2-3 and Comparable Zion Calculations	6
2. ECCS Comparative Information	7

SUMMARY OF LOCE L2-2/L2-3 ANALYSIS AND LOFT/ZION PROTOTYPIC STUDY

INTRODUCTION

To date, two 200% double-ended cold leg break experiments have been completed in the LOFT Power Ascension Test Series. Table 1 contains an abbreviated but pertinent initial conditions comparison list for the two experiments, LOCE L2-2 and LOCE L2-3. LOCE L2-3 was conducted with maximum linear heat generation rate, core fluid temperature rise (ΔT), and system pressure characteristic of the normal operating conditions of a commercial pressurized water reactor (PWR). The thermal behavior of the core in both experiments was dominated by a self-induced cooling mechanism which occurred soon after experiment initiation. The dominance of this phenomena versus current licensing calculation restrictions raises the question of the prototypicality of the LOFT results. The ensuing discussion summarizes both an analysis of the most significant experimental results and a prototypic study of the LOFT results relative to ZION, a commercial PWR. ZION is similar to TROJAN, the commercial PWR to which LOFT was scaled.

L2-2/L2-3 ANALYSIS

The two LOFT experiments had identical event chronologies, as seen in Figure 1. The difference in parameter magnitudes and event occurrence times were consistent with the difference in core power and ΔT initial conditions, listed in Table 1. Measured peak cladding temperature (PCT), 789 K in L2-2 and 914 K in L2-3, occurred during blowdown, the depressurization phase of the transient. Both transients were self-limiting, that is, fluid within the system cooled the core prior to ECC injection.

The core thermal response was closely coupled to the system and resulting core hydraulics during blowdown. The cold leg mass flow balance, seen in Figure 2, produced the most dominant hydraulic

effect. The core inlet flow reversed immediately after experiment initiation. Hot fluid from the core migrated through the lower plenum and downcomer into the broken loop cold leg. The hot fluid arrival in the broken loop cold leg dramatically reduced the mass flow starting at 2.5 s. The intact loop flow, sustained by the operating pumps, exceeded the broken loop flow for 2 s, causing more fluid to enter the downcomer than was expelled through the broken leg. The result was enhanced positive core flow and the influx of high density two-phase fluid, a density wave, which cooled the core. Evidence of the density wave is shown in the self-powered neutron detector (SPND) response in Figure 3. The decrease in negative SPND output was caused by the combined effects of local gamma flux attenuation and an increase in the delayed neutron flux. The density wave caused both of these flux changes. Cladding temperatures did not return to their previous maxima before the core was quenched by emergency core coolant system (ECCS) fluid, as seen in Figure 1.

ECC fluid delivery did not vary significantly with core power as shown in Table 2. Included are data from Experiment L1-5, an isothermal LOFT experiment. The data from L1-5 and L2-2 are essentially identical. In L2-2, evidently, the energy supplied by the nuclear powered core was removed earlier in the transient, confirming the earlier core rewetting measured by the fuel cladding external thermocouples. In L2-3, the increase in stored thermal and fission product decay energies significantly increased the maximum temperature during reflood, which changed the axial rewetting pattern and extended the transient duration from 45 to 55 s, an increase of 22%.

Because of the relatively mild cladding temperatures, no fuel cladding deformation occurred. This result was confirmed by visual inspection after L2-3; consequently, the core will be used for the next test series. Figure 4 shows that the measured cladding temperatures were well below deformation temperature levels.

LOFT/ZION PROTOTYPIC STUDY

LOFT experiments are not demonstration experiments for a full-scale, commercial PWR. However, the results just analyzed raise the question of prototypicality, as current licensing calculation requirements in 10 CFR 50.46, Appendix K prohibit a blowdown rewet even if the predicted core hydraulics are favorable.

Blowdown calculations^a at conditions comparable to LOFT LOCEs L2-2 and L2-3, but characteristic of ZION, were performed to study the prototypical question. Table 1 contains a comparison of the LOFT/ZION initial conditions.

Figures 5 and 6 compare the calculated ZION hot pin and experimentally measured LOFT fuel cladding temperatures during blowdown. In both instances, blowdown PCTs in LOFT are greater than ZION, that is, LOFT temperatures are somewhat conservative to those in its commercial PWR counterpart. To determine the reasons for this trend in cladding temperature, the system and core hydraulics of LOFT and ZION were compared considering

- (1) The initial conditions
- (2) The difference in scale between the two systems
- (3) The system response during a LOCA blowdown, principally, the effect of the cold leg mass flow balance.

In Figures 7, 8, and 9, LOFT L2-2 measured mass flow data are compared with ZION mass flow calculations scaled by the total system volume ratio. In Figure 7, the ZION scaled broken loop cold leg mass

a. Performed using RELAP4/MOD6, Idaho National Engineering Laboratory Configuration Control Number H001184B.

flow overlays LOFT data, as the LOFT break areas were scaled by the total system volume ratio. Figure 8 compares the intact loop(s) cold leg mass flows. Matching initial conditions and the scaling between the two systems causes the ZION mass flow to be 45% greater than LOFT for 5 to 6 s after rupture. The consequence of the greater scaled intact loop(s) flows is shown in Figure 9 which compares the scaled ZION cold leg mass flow balance to LOFT. The net mass per unit total system volume supplied to the ZION downcomer is 3 times that in LOFT, as determined by integrating the positive area under the curves early in blowdown. However, the fluid entering the reactor vessel from the intact loop(s) initially mixes only with fluid in the downcomer and lower plenum before entering the core. If the mass entering the downcomer is scaled to the volumes containing the fluid with which it initially mixes, the multiplier becomes 3.7. Thus, 3.7 times more mass per unit downcomer volume plus lower plenum volume enters the ZION downcomer than LOFT. Although not shown, the ZION/LOFT comparisons for LOCE L2-3 are similar to the L2-2 comparisons. These comparisons reveal that a greater hydraulic rewetting potential exists in ZION than in LOFT.

The greater rewetting potential in ZION affects the core inlet parameters. Due to the absence of core inlet flow instrumentation in LOFT, LOFT RELAP4/MOD6 calculations^a were used to compare with the ZION calculations. The LOFT system hydraulics have been shown previously to be predicted quite accurately by RELAP4/MOD6. In Figure 10, the core positive inlet mass velocity ratio is about 3 or more for the first 8 s. The mass velocity ratio prior to rupture is 3 due to initial conditions and scaling considerations. The large ratio early in time indicates positive core flow resumes in ZION prior to LOFT, which is consistent with the data in Figure 9. The ZION core inlet fluid density is about twice or more the value in LOFT as shown

a. Performed using RELAP4/MOD6, Idaho National Engineering Laboratory Configuration Control Numbers H001184B and H007284B for LOCEs L2-2 and L2-3, respectively.

in Figure 11. Thus, compared to LOFT, the greater hydraulic rewetting potential in ZION produces a greater rewetting influence at the ZION core inlet, as indicated by the mass velocity and fluid density ratios.

These comparisons demonstrate that hydraulic differences, which would influence core rewetting during blowdown, are consistent with the initial conditions, the difference in scale between the two systems, and the mass flow balance in the cold legs. Consequently, the LOFT results, relative to a commercial PWR, conservatively scale the dominant hydraulic phenomena which lead to core rewetting during blowdown for the large break experiments run to date. Such a conclusion supports the credibility of the cladding temperature comparisons in Figures 5 and 6 and the conclusion that LOFT results provide a realistic if not conservative indication of fuel cladding temperatures during blowdown of a commercial PWR.

TABLE 1. INITIAL CONDITIONS FOR LOCE L2-2 AND LOCE L2-3
AND COMPARABLE ZION CALCULATIONS

	<u>L2-2</u>	<u>ZION</u>	<u>L2-3</u>	<u>ZION</u>
Maximum linear heat generation rate (kW/m)	26.4	25.6	39.4	39.4
Core power (MW)	24.88	2 296.6	36.7	3 540.0
Primary coolant mass flow (kg/s)	194.2	18 395.0	199.8	18 395.0
Hot-to-cold leg temperature difference (K)	22.7	23.9	32.2	35.8
Cold leg temperature (K)	557.7	549.8	560.7	549.8
System pressure (MPa)	15.64	15.42	15.06	15.43

TABLE 2. ECCS COMPARATIVE INFORMATION

	L1-5	L2-2	L2-3
Accumulator injection initiation (s)	19	18	17
First indication in down-comer of ECCS fluid (s)	24	24	25
Reflood rate (m/s)	0.12 ± 0.02	0.12 ± 0.02	0.10 ± 0.02
Bypass (%)	30 ± 4	32 ± 3	36 ± 4
Core volume reflooded (s)	59	55	55
Axial rewetting pattern	Bottom-to-top	Bottom-to-top	Bottom-top-middle
Last rewet (s)	45	45	55
Maximum cladding temperature during reflood (K)	515	665	850

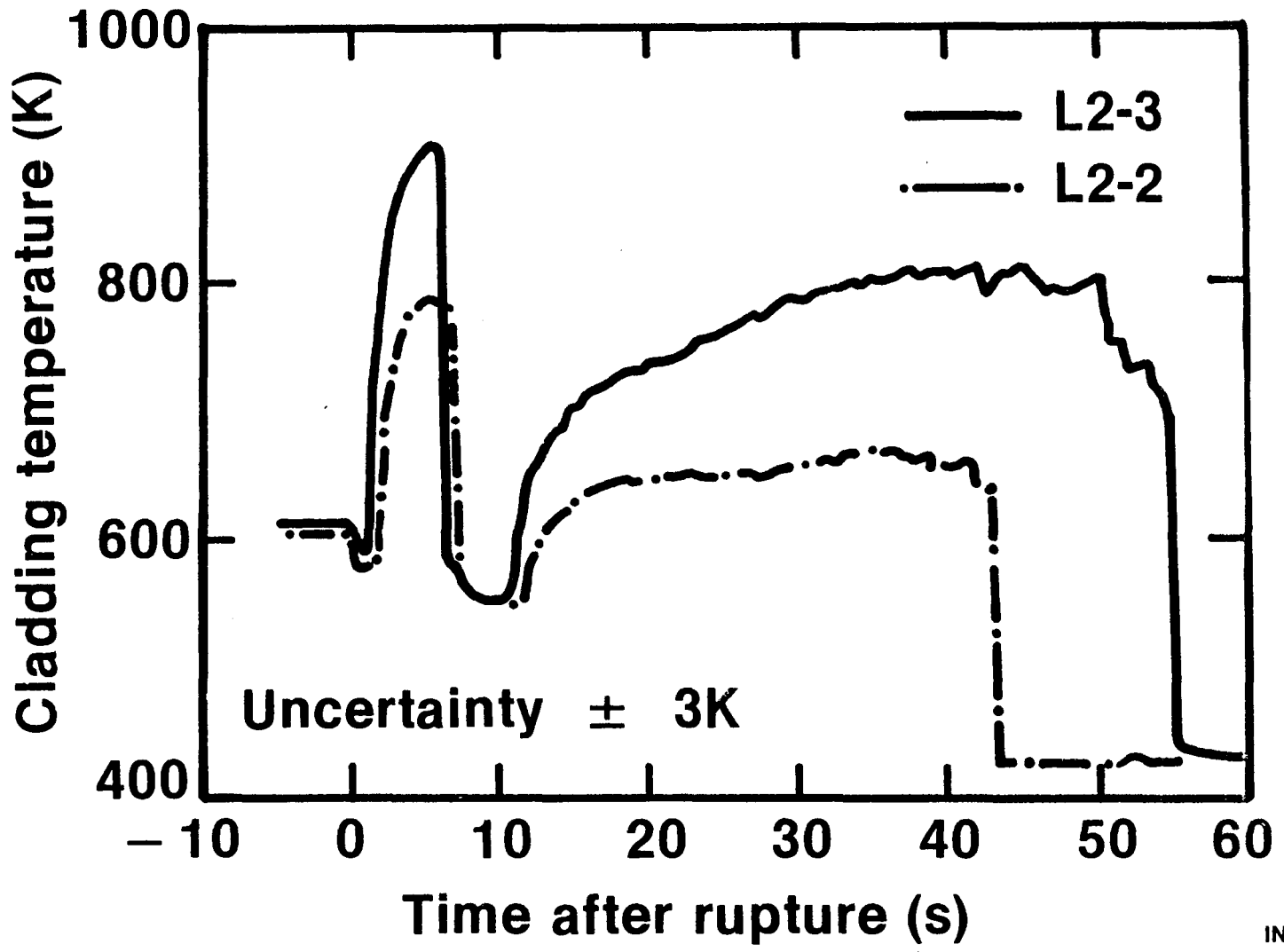


Figure 1. L2-2/L2-3 cladding temperature comparison.

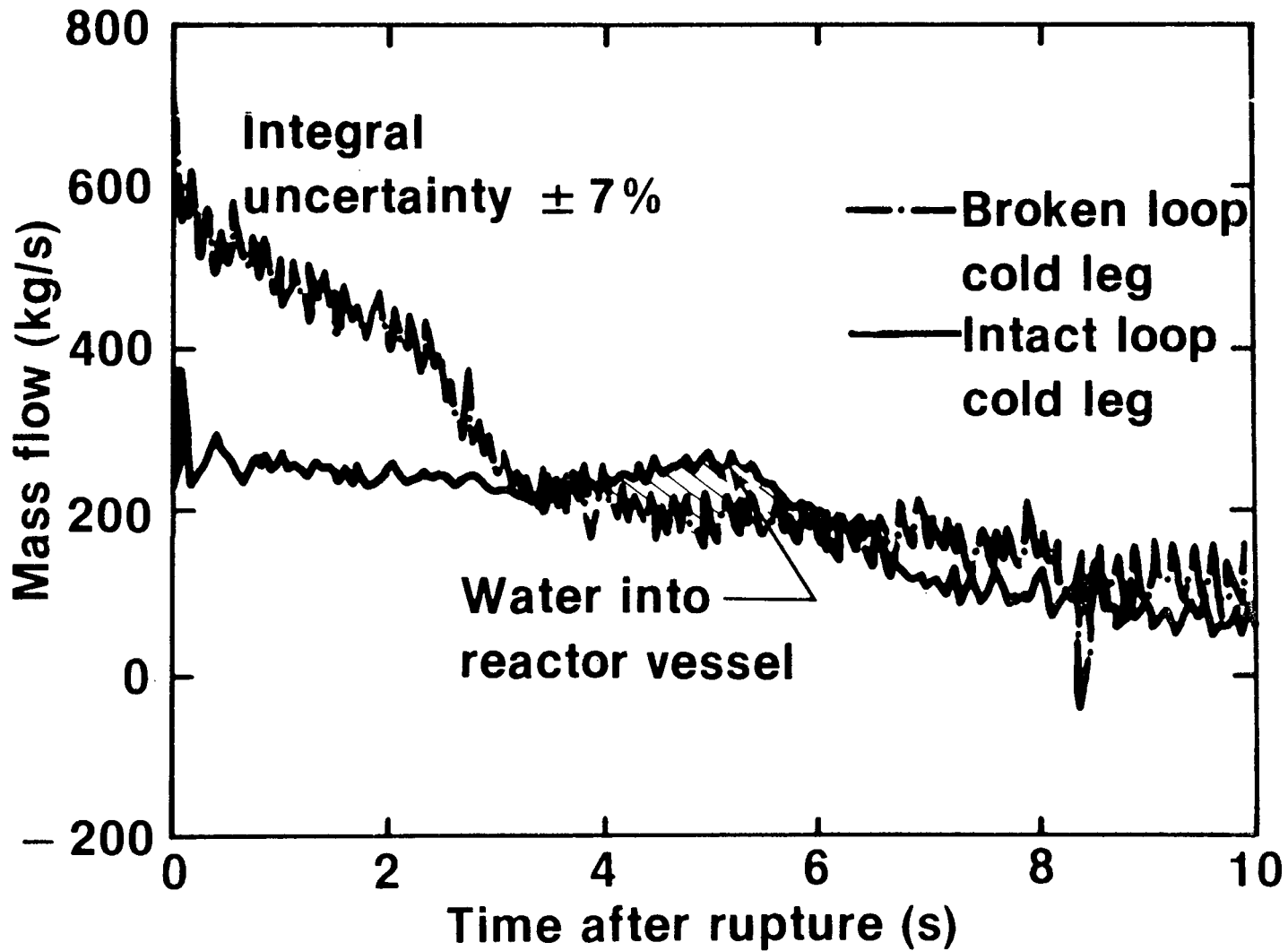
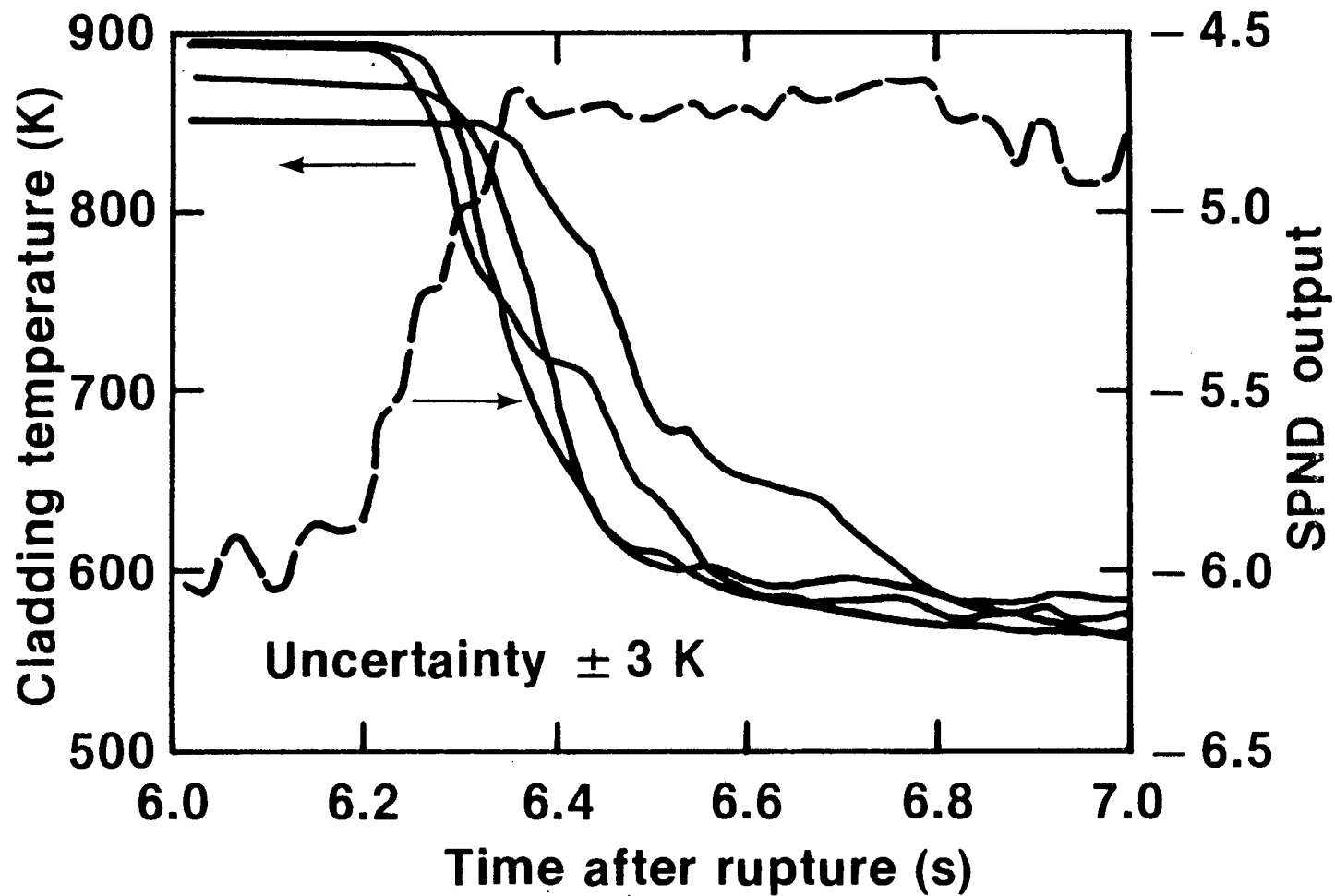


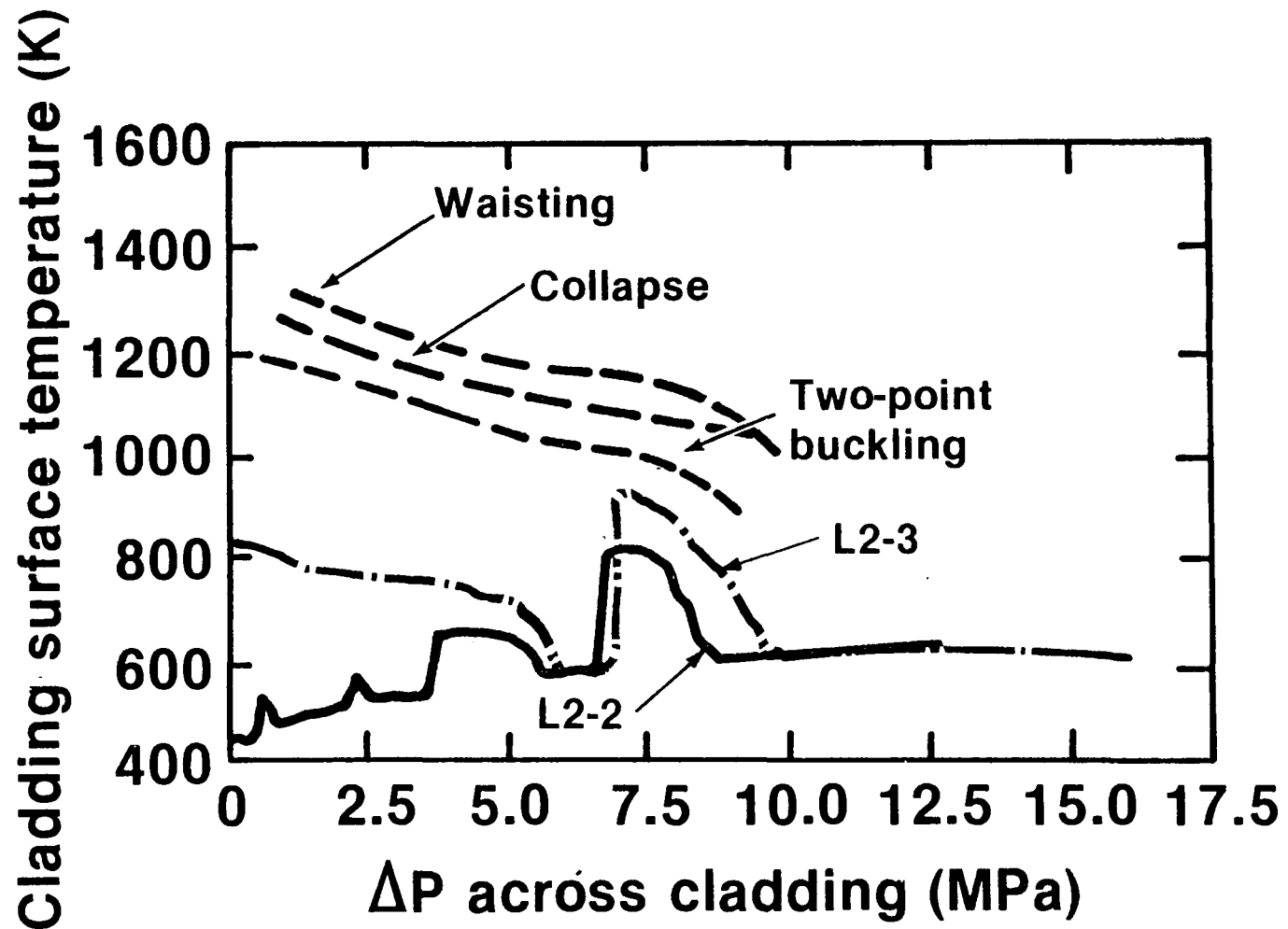
Figure 2. Cold leg mass flows.



— Cladding temperatures
 - - - SPND output

INEL-S-19 877

Figure 3. L2-3 cladding temperature versus SPND output.



INEL-S-18 315

Figure 4. Cladding deformation.

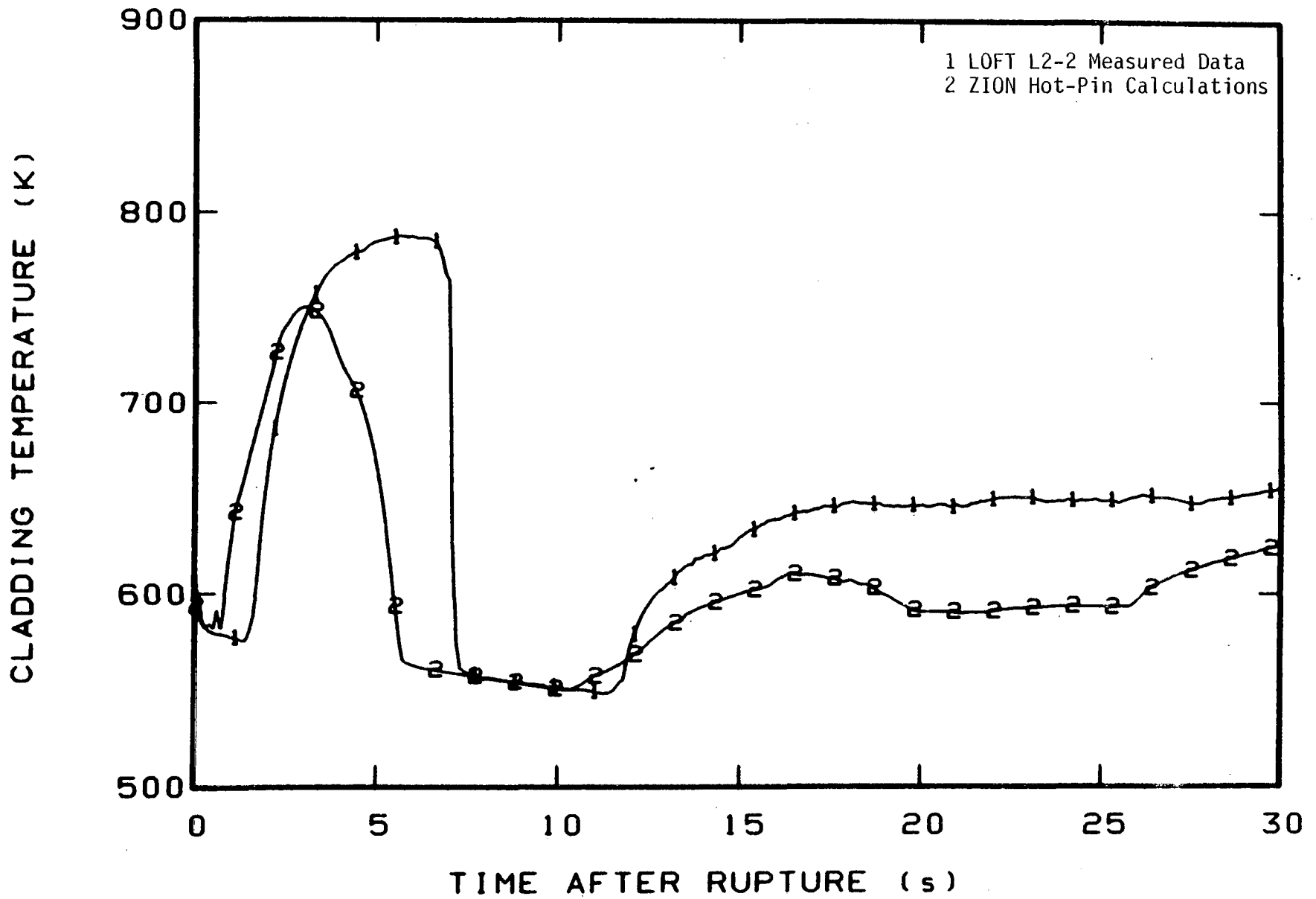


Figure 5. Fuel cladding temperature comparison.

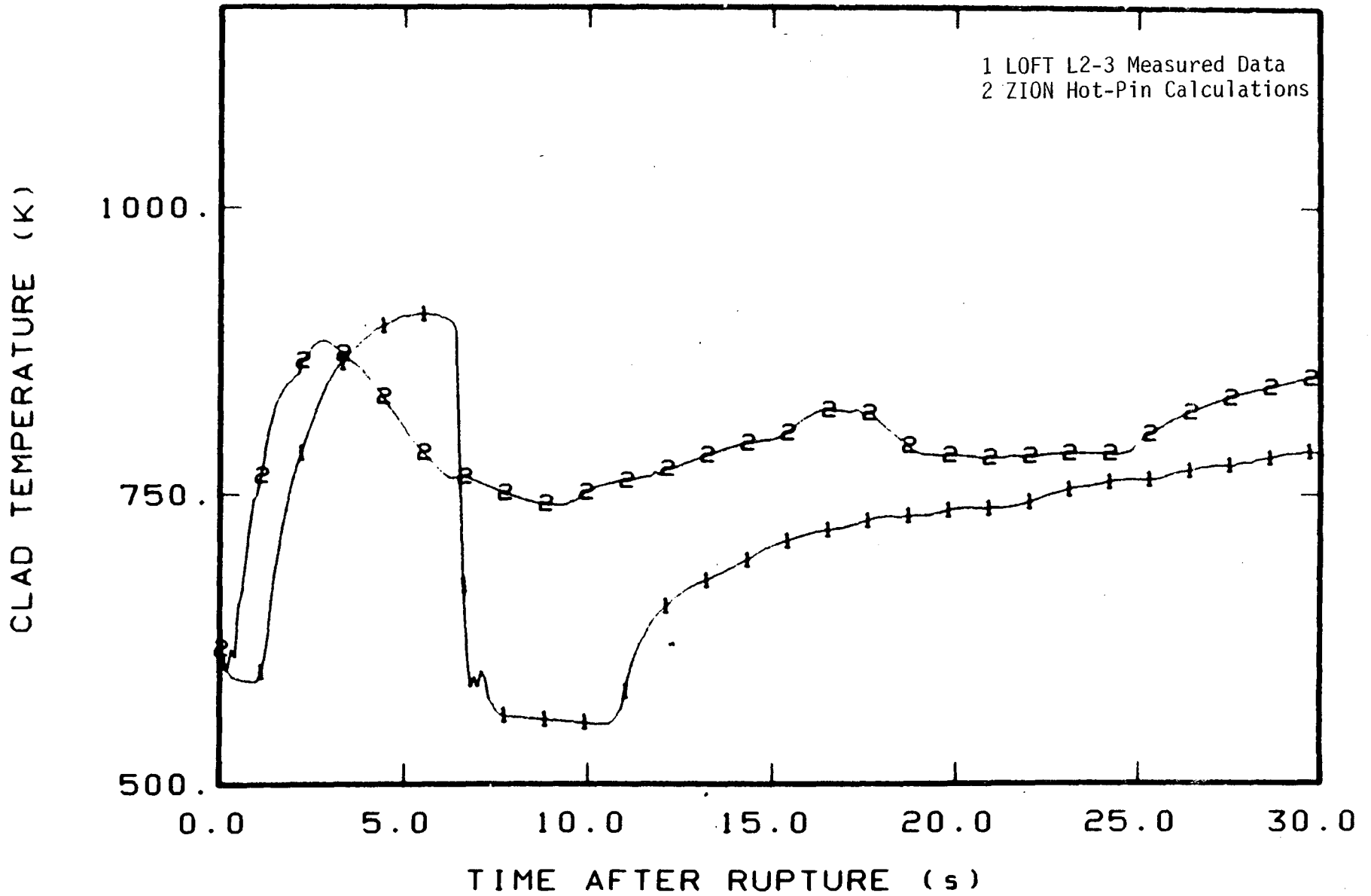


Figure 6. Fuel cladding temperature comparison.

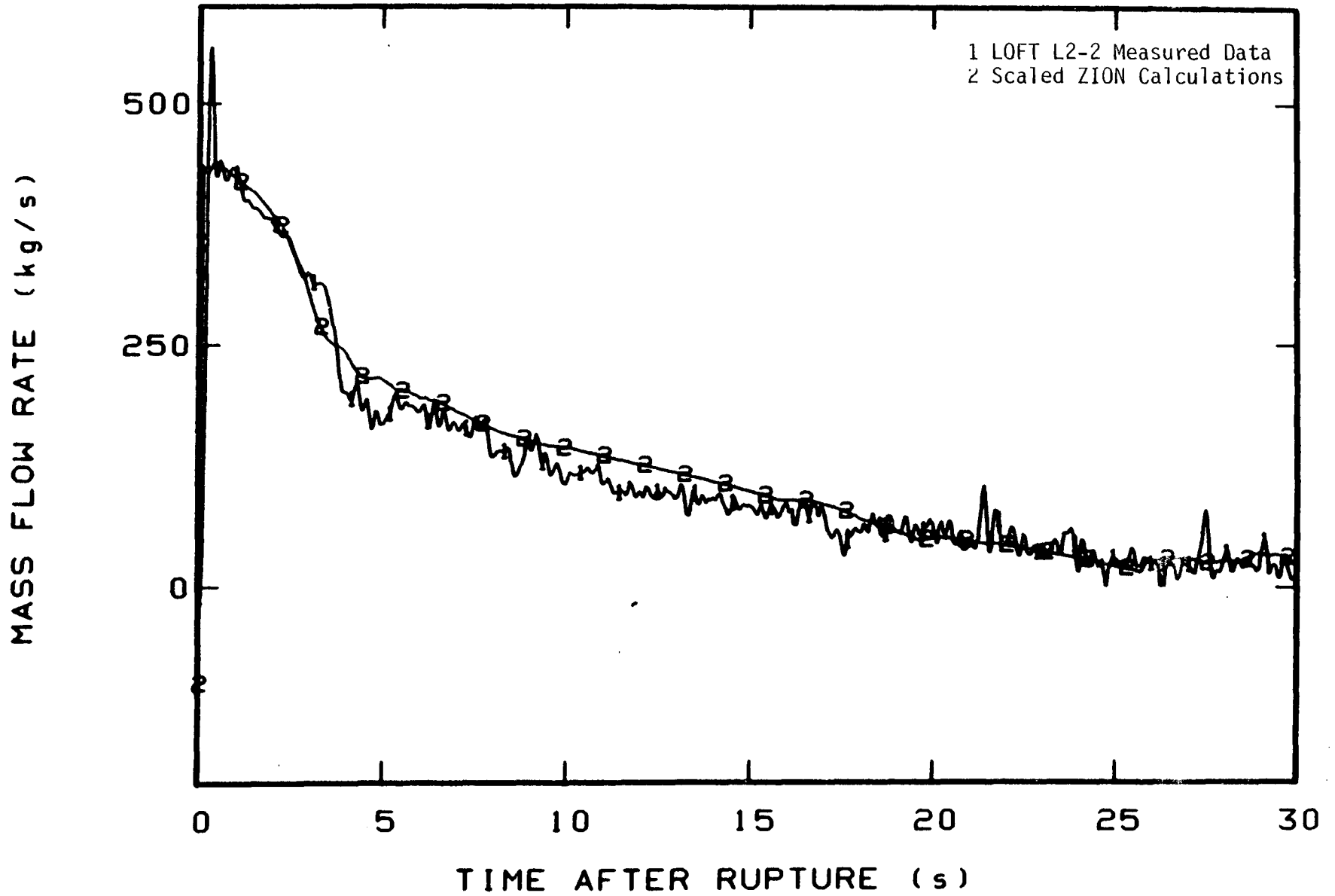


Figure 7. Broken loop cold leg mass flow comparison.

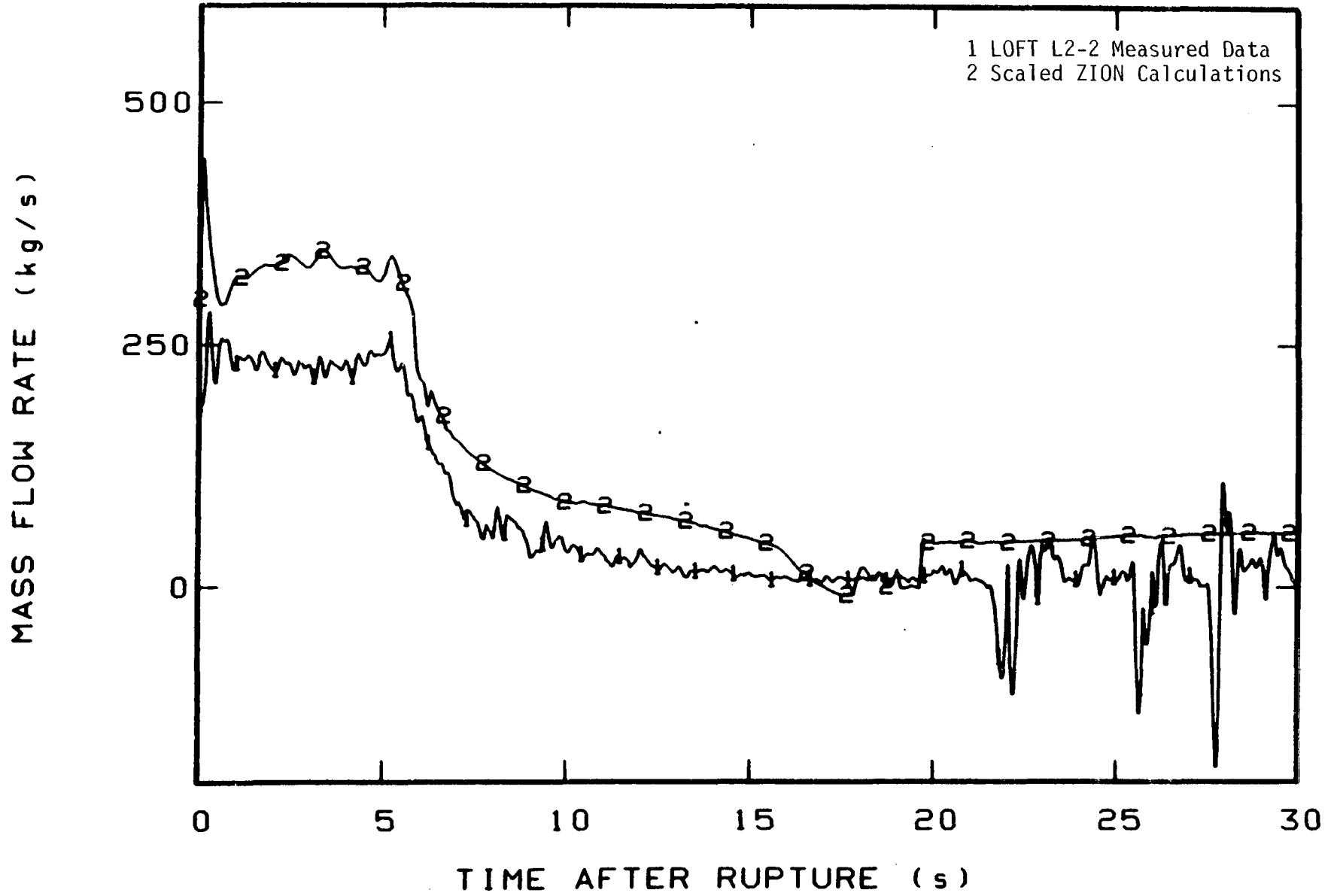


Figure 8. Intact loop(s) cold leg mass flow comparison.

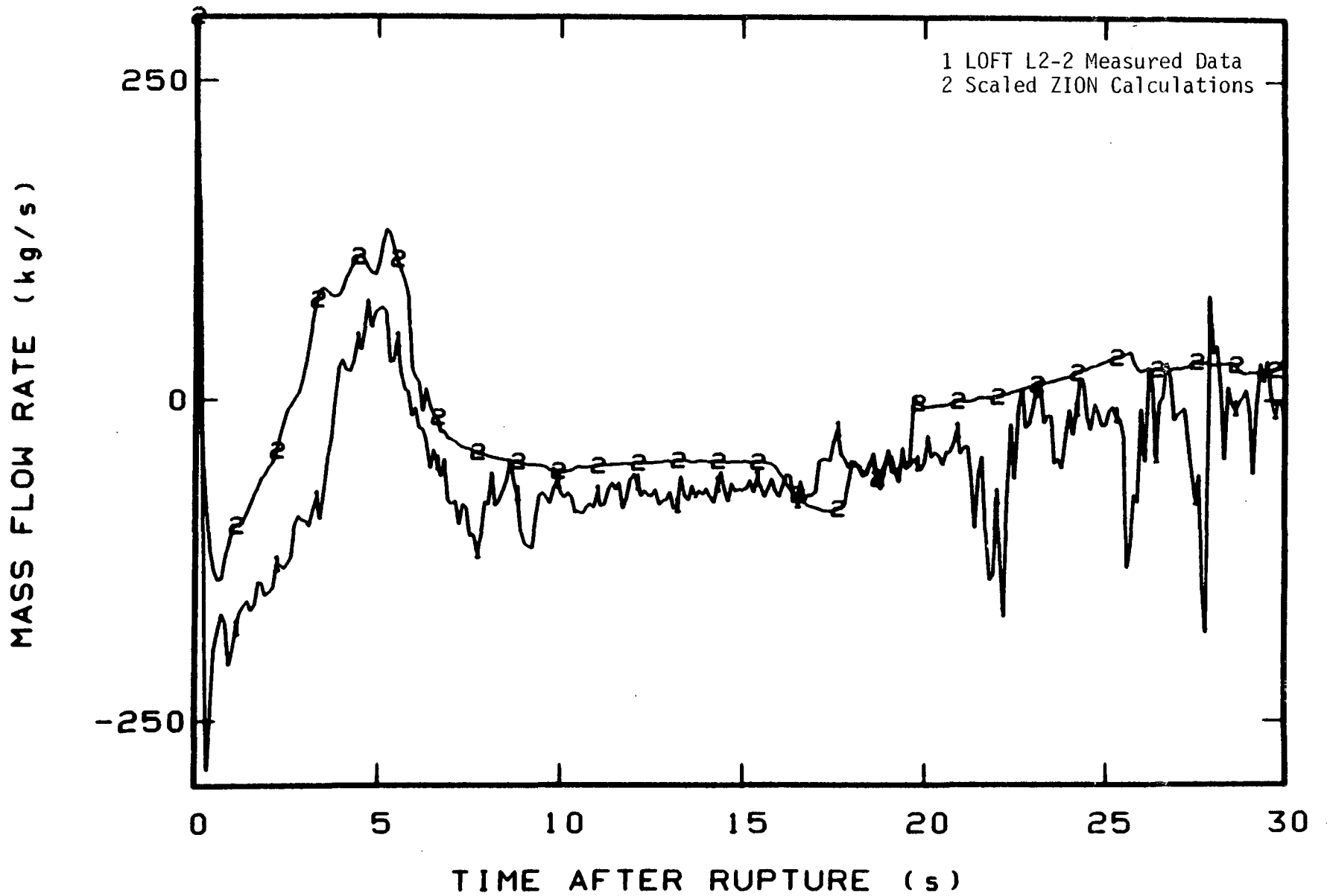


Figure 9. Comparative cold leg mass flow balance (Intact--Broken).

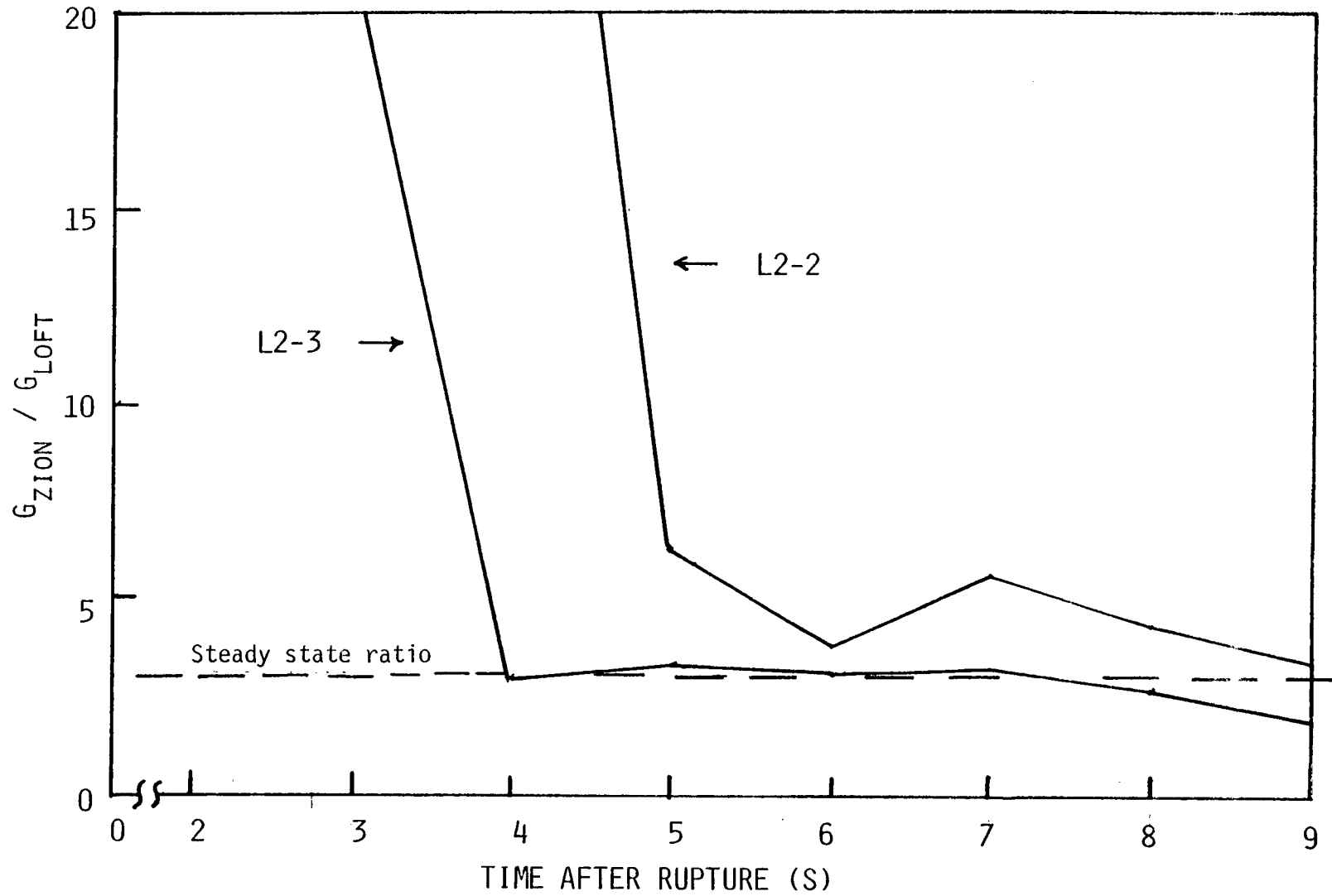


Figure 10. Core inlet mass flux ratio from RELAP4/MOD6 calculations.

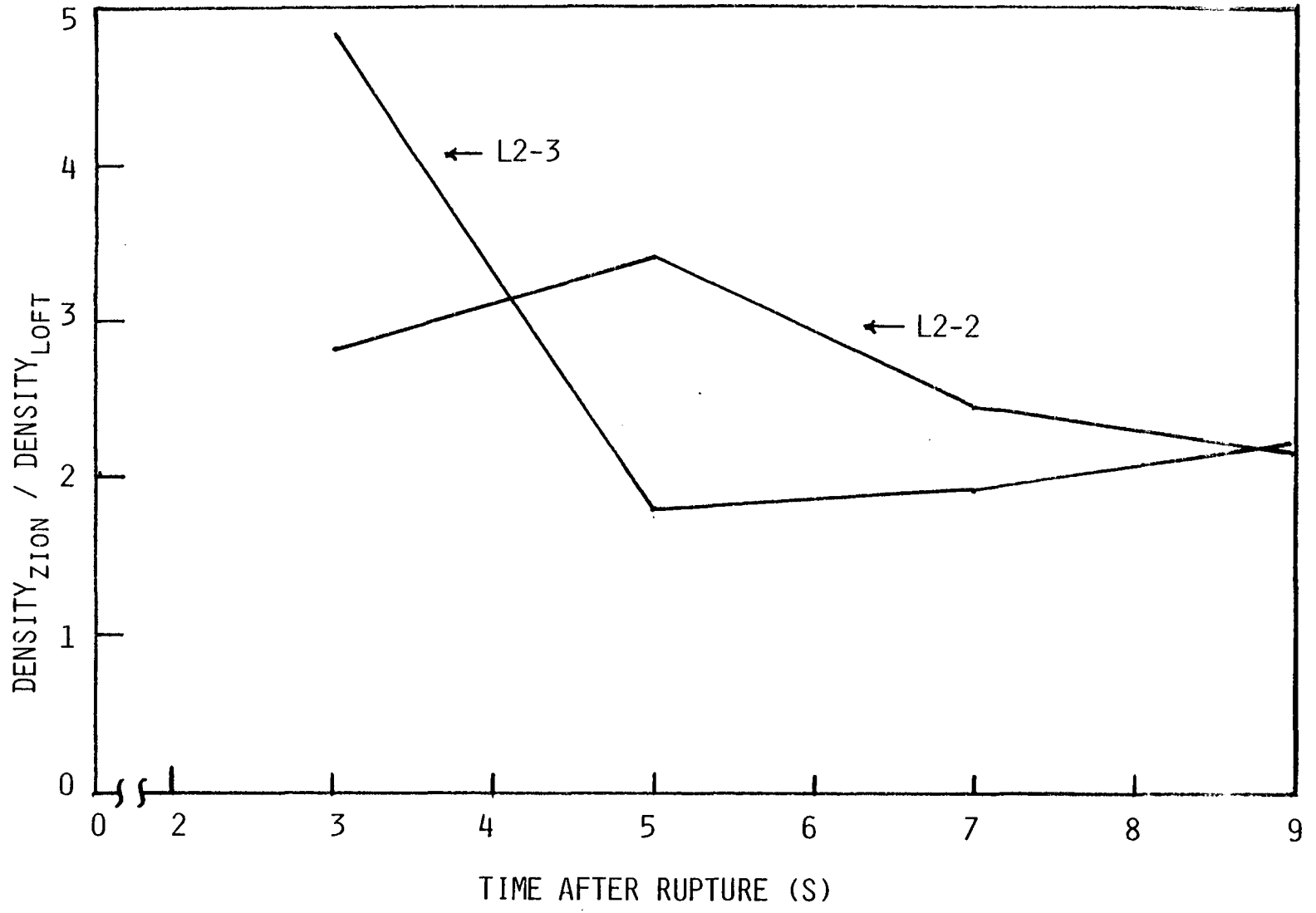


Figure 11. Core inlet density ratio from RELAP4/MOD6 calculations.

A DISCUSSION OF DIFFERENT ANALYTICAL APPROACHES TO PREDICTING REWET
PHENOMENA IN LOSS-OF-COOLANT EXPERIMENTS
(RELAP4/MOD6 and TRAC-P1A Predictions of LOFT Experiment L2-3)

R. A. Nelson

CONTENTS

INTRODUCTION	1
RELAP4/MOD6 AND TRAC-P1A CALCULATIONS	2
SUMMARY AND CONCLUSIONS	5

FIGURES

1. RELAP4/MOD6 boiling curve	7
2. RELAP4/MOD6 blowdown heat transfer surface	8
3. RELAP4/MOD6 calculated cladding temperature at the hot spot	9
4. RELAP4/MOD6 calculated mass flux at the hot spot	10
5. RELAP4/MOD6 calculated quality at the hot spot	11
6. TRAC-P1A boiling curve	12
7. Effects of the Iloeje minimum film boiling correlation on the TRAC-P1A boiling curve	13
8. Effects of RELAP4 critical heat flux correlation on TRAC-P1A	14
9. Effects of TRAC-P1A critical heat flux correlations on RELAP4/MOD6	15
10. Effects of TRAC-P1A critical heat flux correlation on RELAP4/MOD6 calculated cladding temperature	16
11. Comparison of fluid conditions in post-critical heat flux data base and LOFT calculations	17
12. Comparison of fluid conditions in post-critical heat flux data base and ZION calculations	18

A DISCUSSION OF DIFFERENT ANALYTICAL APPROACHES TO PREDICTING REWET
PHENOMENA IN LOSS-OF-COOLANT EXPERIMENTS
(RELAP4/MOD6 and TRAC-P1A Predictions of LOFT Experiment L2-3)

INTRODUCTION

The core rewet phenomena observed in recent LOFT Loss-of-Coolant Experiments (LOCE) L2-2 and L2-3 were not adequately predicted by either RELAP4/MOD6^{a,b} or TRAC-P1A; however, by modifying TRAC-P1A to include the Iloeje minimum film boiling correlation, the experimentally observed rewet phenomena were predicted. A study is currently underway to determine what physical phenomena must be accounted for to obtain a correct analytical technique to accurately predict the core rewet phenomena observed in experiments such as LOFT LOCEs L2-2 and L2-3. The first phases of that study involve determining the reasons why RELAP4/ MOD6 and TRAC-P1A did or did not predict the experimentally observed rewets. This discussion explains what has been learned to date, during this first phase of the study.

Three calculational aspects of the codes are postulated to have caused the disparity between predicted and measured fuel rod cladding temperature response for LOCEs L2-2 and L2-3:

1. The initial fuel rod stored energy
2. The hydraulic calculation
3. The heat transfer surface.

-
- a. RELAP4/MOD6, Update 4, Idaho National Engineering Laboratory Configuration Control Number C0010006.
 - b. The version of RELAP4/MOD6 used for the experiment prediction for LOCE L2-3 is under Idaho National Engineering Laboratory Configuration Control Numbers H003384B and H003284B.

The RELAP4/MOD6 fuel rod stored energy and hydraulic calculations have been examined and determined to be reasonable. Although TRAC-P1A did not predict the system hydraulics as well as RELAP4/MOD6, its core hydraulics were similar enough to those of RELAP4/MOD6 to not affect the material presented here. It has been concluded that further investigation on core rewet behavior should be concentrated on gaining an understanding of methods of calculating the basic heat transfer processes.

The objective of this discussion is to provide an understanding of why RELAP4/MOD6 and TRAC-P1A predictions of LOFT LOCE L2-3 did not predict the observed fuel rod cladding rewet while TRAC-P1A plus the Iloeje minimum film boiling correlation prediction did. To obtain this understanding, the initial process is to determine how the post-critical heat flux (CHF) boiling curves are constructed from convective heat transfer correlations in the two computer codes. This knowledge can then be used to explain what physical processes must be accounted for in the analytical modeling to accurately represent the physically observed rewet phenomena.

RELAP4/MOD6 AND TRAC-P1A CALCULATIONS

An essential element of calculating rewet behavior using either RELAP4/MOD6 or TRAC-P1A is in the proper prediction of post-CHF heat transfer as reflected in the calculated boiling curve. The RELAP4/MOD6 post-CHF portion of the boiling curve is constructed by summing the transition and film boiling correlations, as shown in Figure 1. Although a minimum wall superheat, ΔT_{\min} , is implied and can be calculated, it is not generally evaluated. A family of boiling curves would result from varying the quality parameter and could also be plotted. However, the plotting technique developed under the RELAP4/MOD6 development effort results in these boiling curves being represented as three-dimensional with quality as the new variable. This technique has been termed the heat transfer surface approach and is shown in Figure 2 for a given set of fluid conditions which exist at 7

seconds in the RELAP4/MOD6 prediction of the LOFT LOCE L2-3 hot spot. This surface can be considered to be recalculated at each time step of the calculation as a function of the new hydraulic conditions.

With this understanding of the RELAP4/MOD6 heat transfer, the failure of RELAP4/MOD6 to predict rewet can now be explained. Figures 3, 4, and 5 represent the hot spot wall temperature, mass flux, and quality, respectively, for the RELAP4/MOD6 prediction of LOFT LOCE L2-3. From these figures, the cooldown shown for the hot spot wall temperature at about 4 seconds is seen to be associated with periods when the core flow is in one direction long enough and liquid mass in the lower plenum is sufficient to produce a decrease in the core quality at the hot spot. This hydraulic phenomenon is discussed in detail with respect to the measurements in the companion paper by Dr. Linebarger. In terms of the convective heat transfer, the effects of these hydraulics can best be visualized by evaluating the RELAP4/MOD6 heat transfer surface as a function of time and denoting the hot spot true temperature and quality on the cladding surface. Evaluation is done conceptually by plotting an approximate loci of points on Figure 2 which represents the hot spot surface temperature and quality as a function of time. This calculated visualization is not exact since the heat transfer surface moves somewhat as a function of time, but it does convey the principle. From this visualization, an understanding of why a rewet is not predicted during the RELAP4/MOD6 prediction at about 4 to 6 seconds is obtained. For example, an additional decrease in predicted quality of 20% would have placed the calculation well into transition boiling so that a rewet would have probably occurred. This is not meant to imply, however, that the hydraulic prediction is in error. The failure to predict the rewet can, in fact, come from any combination of the hydraulics, the convective heat transfer, and/or the fuel pellet-gap modeling, which governs the heat coming into the back of the cladding.

To investigate why TRAC-PIA did or did not predict rewet in the LOCE L2-3 calculation, the manner in which the boiling curves are generated must also be understood. Figure 6 represents a typical

TRAC-P1A boiling curve. The post-CHF region is generated by using the nucleate boiling and the CHF correlations to define q_{DNB} and ΔT_{DNB} . Next, ΔT_{min} and the film boiling correlation are generated through use of the minimum wall superheat correlation and evaluated at ΔT_{min} to yield q_{min} . These two points are then interpolated with respect to wall superheat linearly on a log-log basis to produce the transition boiling portion of the boiling curve.

With this understanding of the TRAC-P1A boiling curve, the two TRAC-P1A predictions of LOCE L2-3 can be discussed. If the temperature at which the rewet should be predicted is now denoted as $\Delta T_{L2-3 \text{ rewet}}$, its relative position on the boiling curve can be shown (see Figure 7). For TRAC-P1A, the ΔT_{min} was defined by the Henry correlation and is less than $\Delta T_{L2-3 \text{ rewet}}$. For this reason, the TRAC-P1A calculation does not predict rewet. The Iloeje correlation of ΔT_{min} , however, is greater than $\Delta T_{L2-3 \text{ rewet}}$ for these hydraulic conditions; therefore, transition boiling is introduced instead of film boiling and a rewet is calculated.

Thus, a basic understanding of why TRAC-P1A did not predict rewet, whereas TRAC-P1A with the Iloeje correlation did is obtained. However, factors other than the minimum film boiling should be considered. As basic to the rewet prediction as Iloeje's ΔT_{min} was, the CHF correlation is just as important. The characteristic of the TRAC-P1A CHF correlation which makes this statement true is its inverse mass flux effect, that is, the critical heat flux increases as mass flux decreases. For the low flow conditions within the core at the time of rewet, this is particularly important. RELAP4/MOD6 however uses a CHF correlation which has a direct mass flux effect, that is, the critical heat flux decreases as mass flux decreases.

Figure 8 then shows conceptually what happens if the RELAP4/MOD6 critical heat flux correlation is used in TRAC-P1A to generate the boiling curve at the time of rewet for the hydraulic conditions present. The heat flux at $\Delta T_{L2-3 \text{ rewet}}$ is reduced and the prediction may or may not predict rewet. Similarly, substitution of the TRAC-P1A CHF

correlation into RELAP4/MOD6^a was hypothesized to produce the effect shown in Figure 9 so that a rewet would be predicted. This substitution was made, and the LOCE L2-3 prediction was repeated with a rewet being predicted as shown in Figure 10. Similar results were also obtained for a recalculation of LOFT LOCE L2-2. Hence, a change in the RELAP4/MOD6 CHF correlation produced results similar to the TRAC-P1A ΔT_{\min} change.

SUMMARY AND CONCLUSIONS

Thus far, an understanding of why RELAP4/MOD6 and TRAC-P1A did not predict rewet and why TRAC-P1A with the Iloeje correlation did has been obtained. RELAP4/MOD6, when modified with the TRAC-P1A critical heat flux correlation, was shown to predict the observed rewets. Also an understanding of how each of these different combinations affects the heat transfer boiling curves or surface has been developed.

In order to evaluate which one of these different heat transfer methods for predicting the rewet of LOCE L2-3 is correct, the available (approximately 4500) post-CHF tube data points, with respect to their mass flux and quality were examined, and the RELAP4-MOD6 prediction of the hot spot hydraulics for LOCE L2-3 was superimposed. This information is shown in Figure 11 and it is evident that no data exist in the region of interest. From Figure 11, the conclusion reached can only be that no (or minimal) data are available to determine what is the correct analytical approach. All the film boiling and transition boiling correlations used in RELAP4/MOD6 and the film boiling correlations in TRAC-P1A were developed from these data, and, therefore, unfortunately the correlations must be used outside their range of assessed applicability for predicting rewet conditions such as those that existed in LOCE L2-3.

a. The RELAP4/MOD6 code as modified by adding the TRAC-P1A CHF correlation is under Idaho National Engineering Laboratory Configuration Control Number H007284B.

If the results examined here are to be related to a commercial PWR, the companion paper by Dr. Linebarger which addresses calculations for the ZION plant can be considered. The rewet predicted by RELAP4/MOD6 for ZION is now understood since the fluid density during the flow up through the core was greater in ZION than in LOFT LOCE L2-3. Therefore, with respect to Figure 2, both the quality and the wall temperature at the hot spot were less, and transition boiling would have been encountered. With respect to the data bank comparison, Figure 12 presents a similar comparison of the ZION predicted hydraulic conditions. Unfortunately the same basic lack of data exists.

On the basis of experience in modeling rewet phenomena with RELAP4/MOD6, the conclusion reached is that the ZION calculations may underestimate the core heat transfer during the time when substantial positive core flow exists. A further conclusion is that additional separate effects tests are needed to broaden the data base, especially in the area of low flow, low quality post-CHF heat transfer.

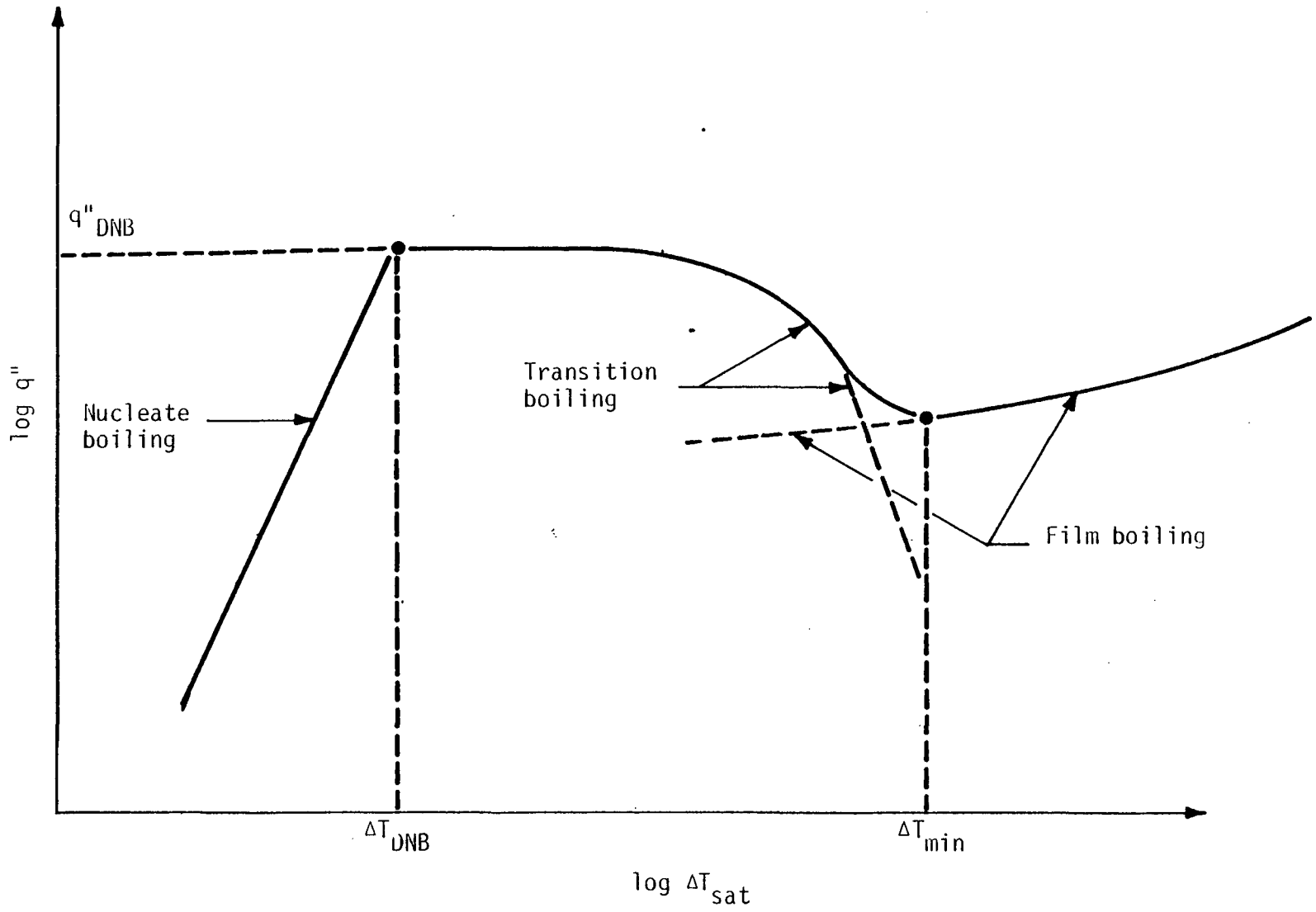


Figure 1. RELAP4/MOD6 boiling curve.

α

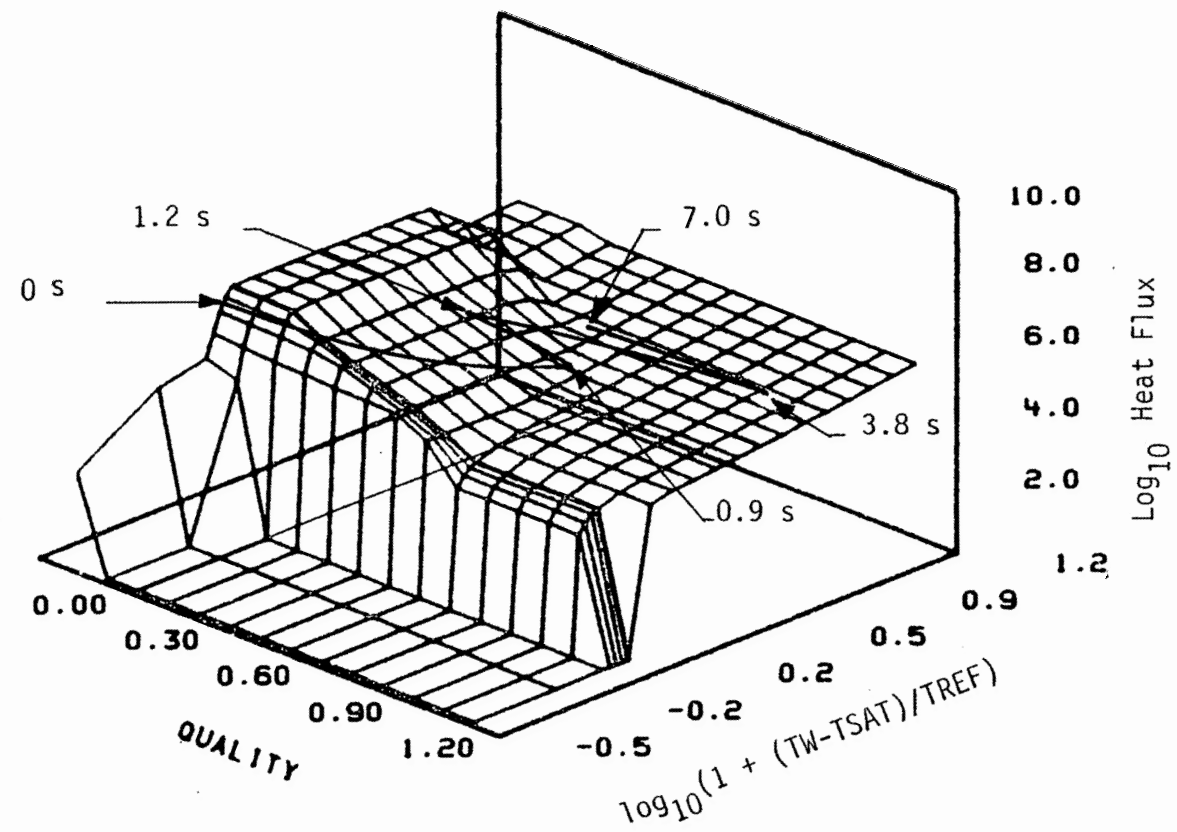


Figure 2. RELAP4/MOD6 blowdown heat transfer surface,

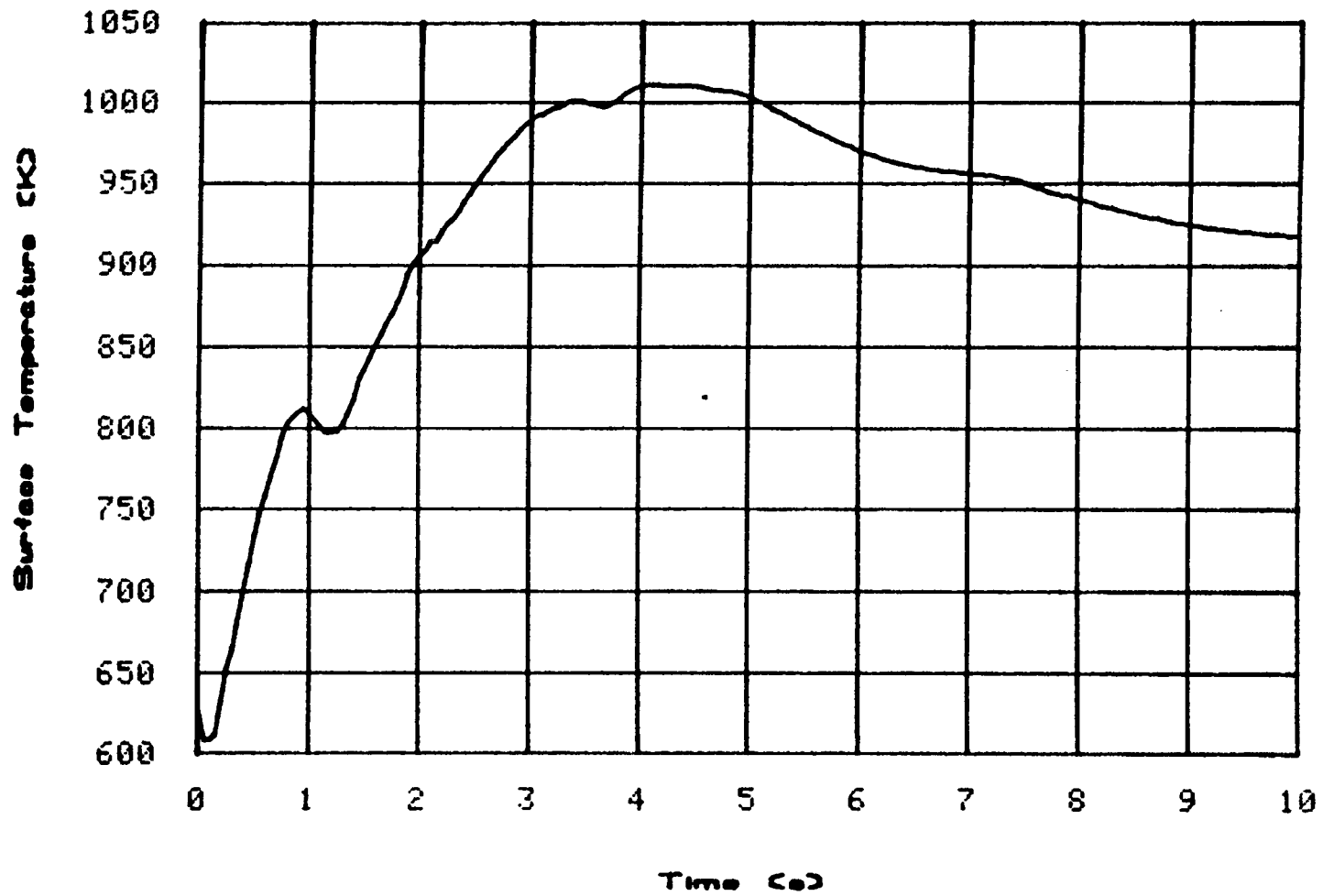


Figure 3. RELAP4/MOD6 calculated cladding temperature at the hot spot.

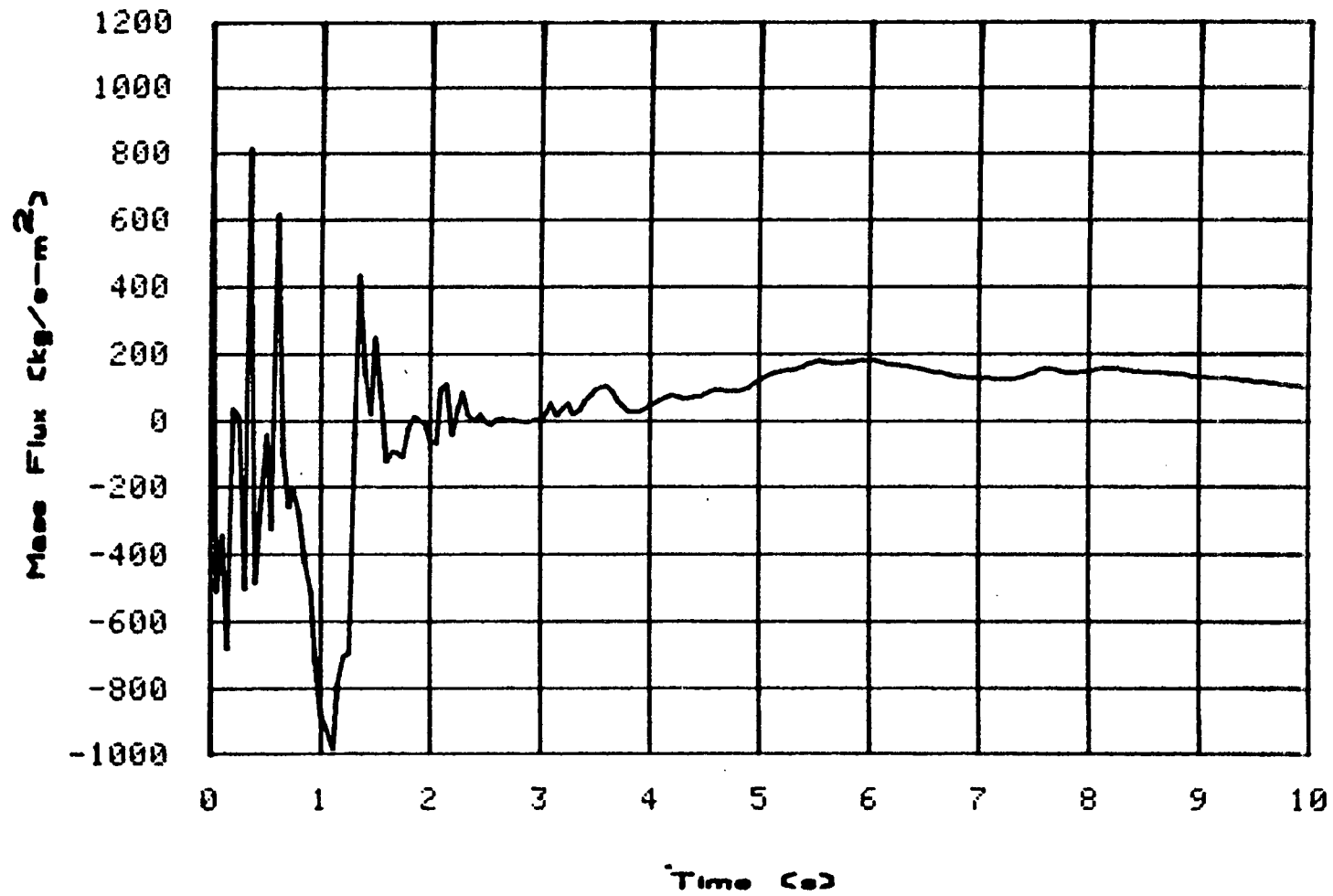


Figure 4. RELAP4/MOD6 calculated mass flux at the hot spot.

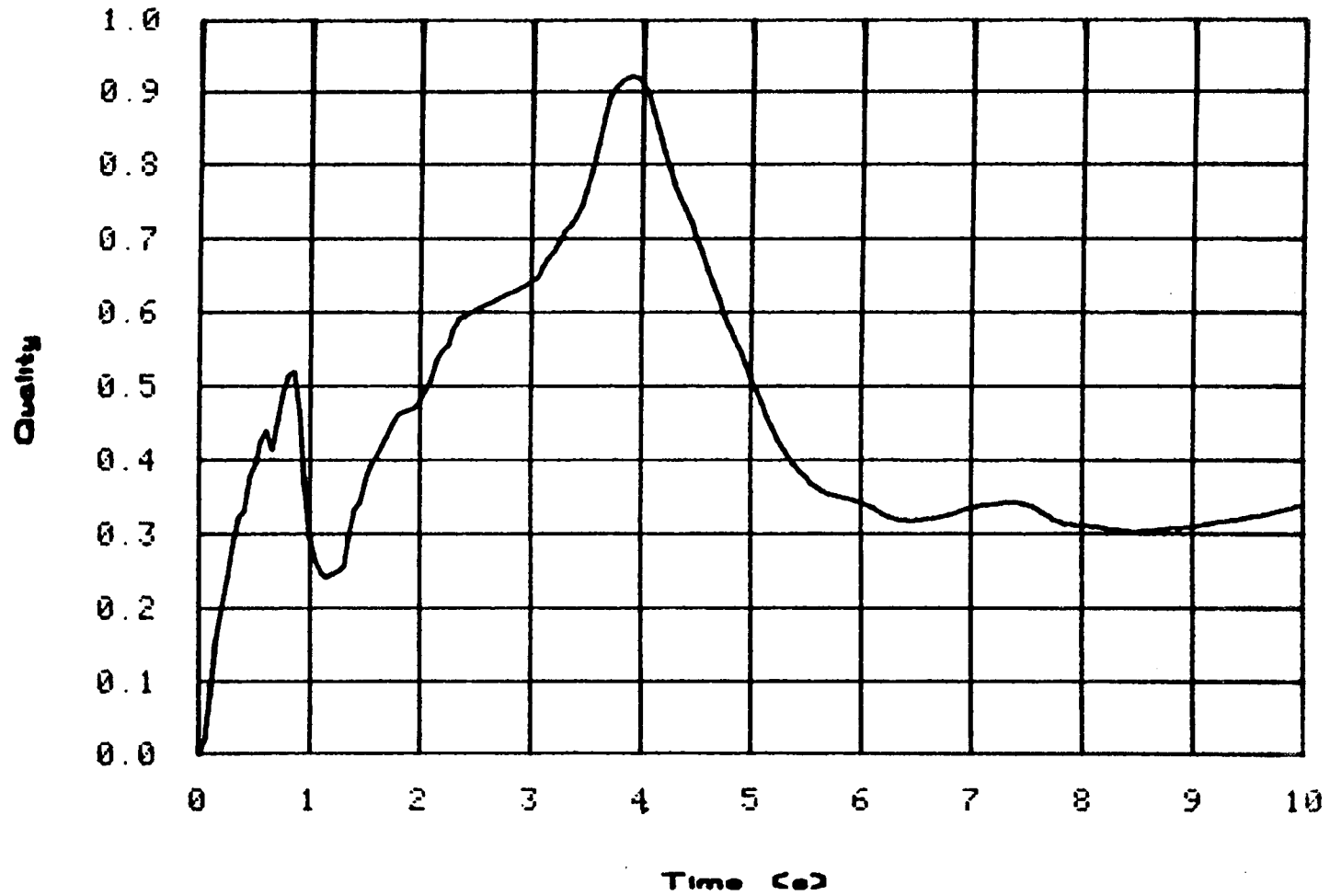


Figure 5. RELAP4/MOD6 calculated quality at the hot spot.

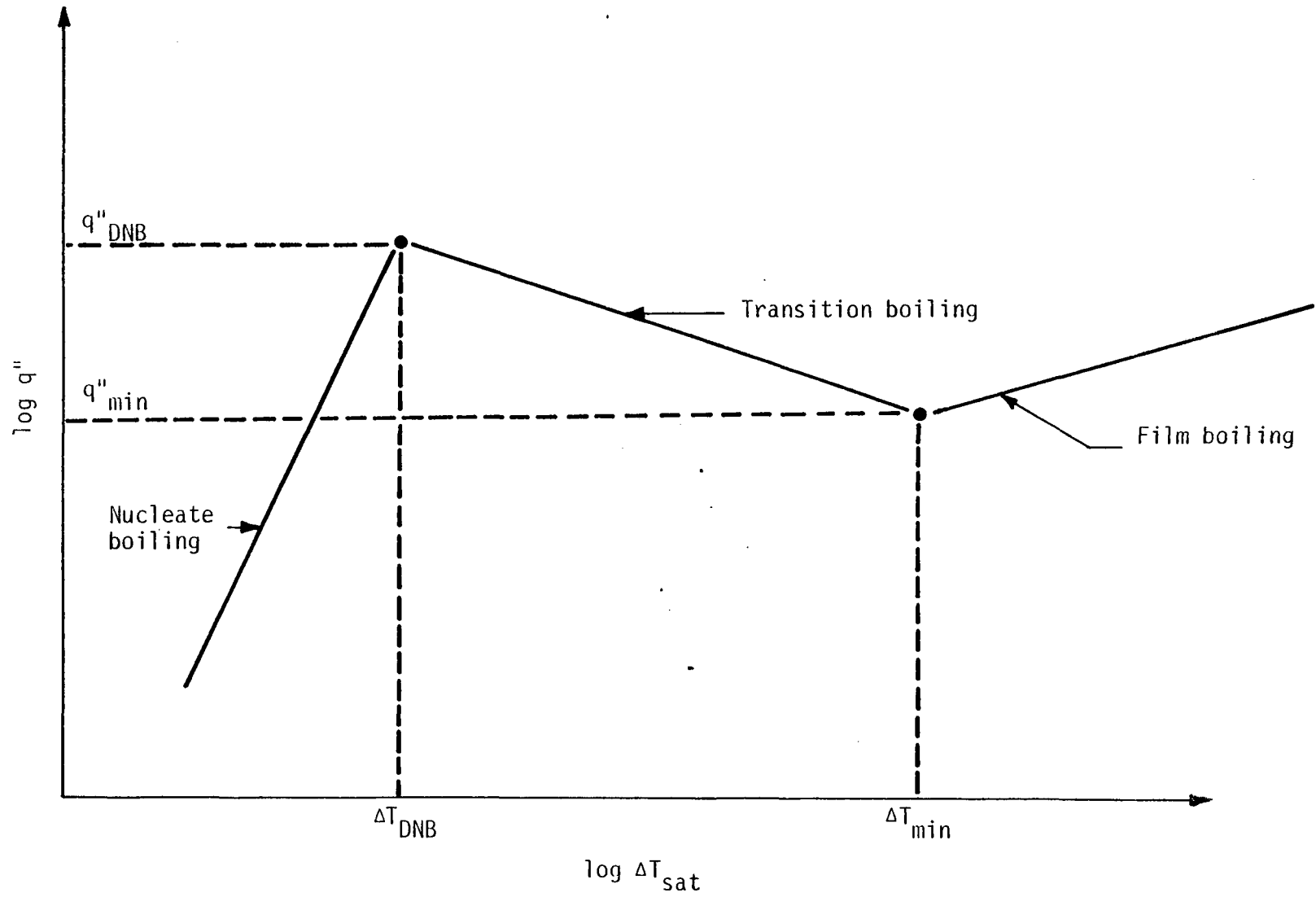


Figure 6. TRAC-P1A boiling curve.

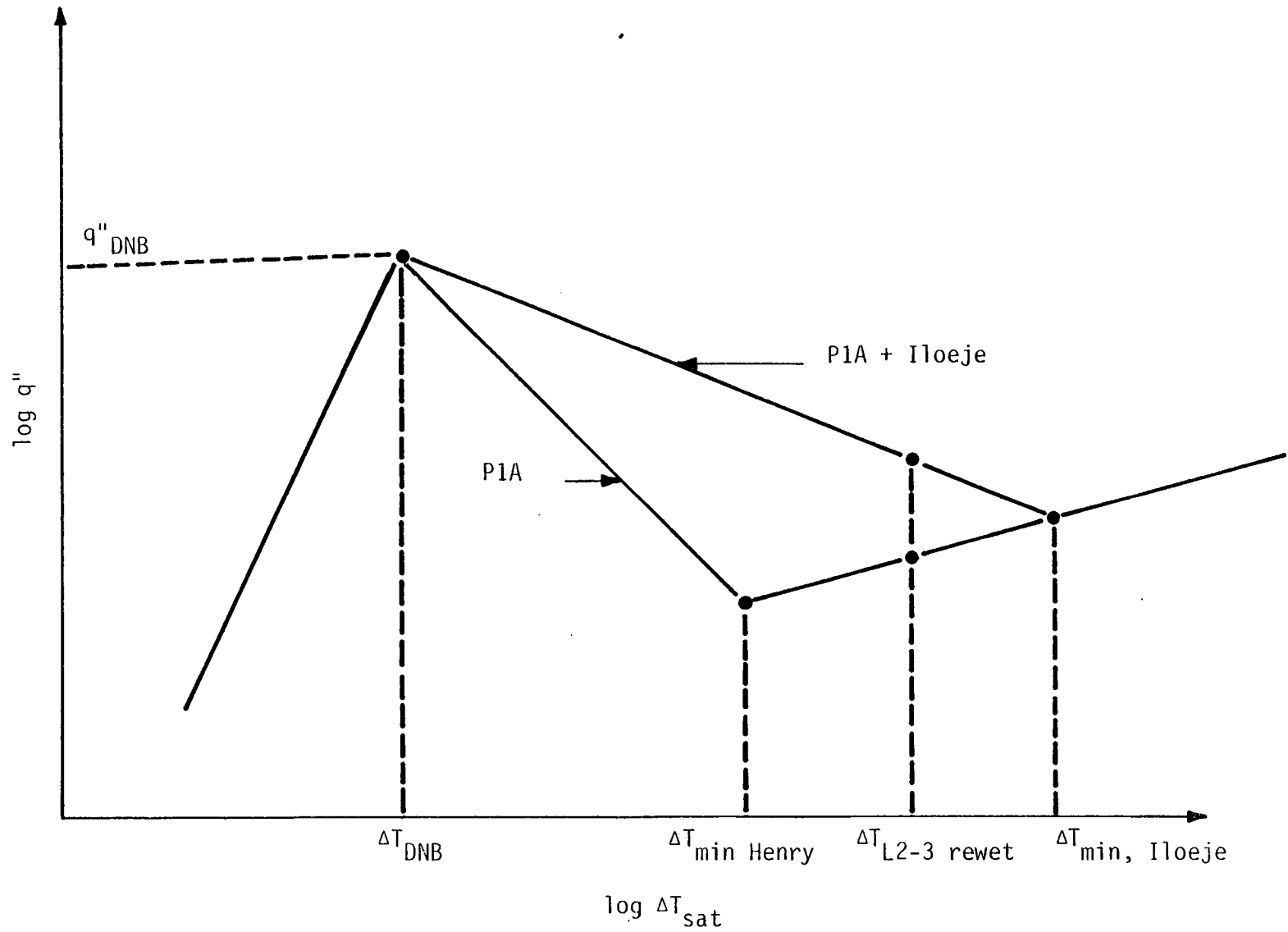


Figure 7. Effects of the Iloeje minimum film boiling correlation on the TRAC-P1A boiling curve.

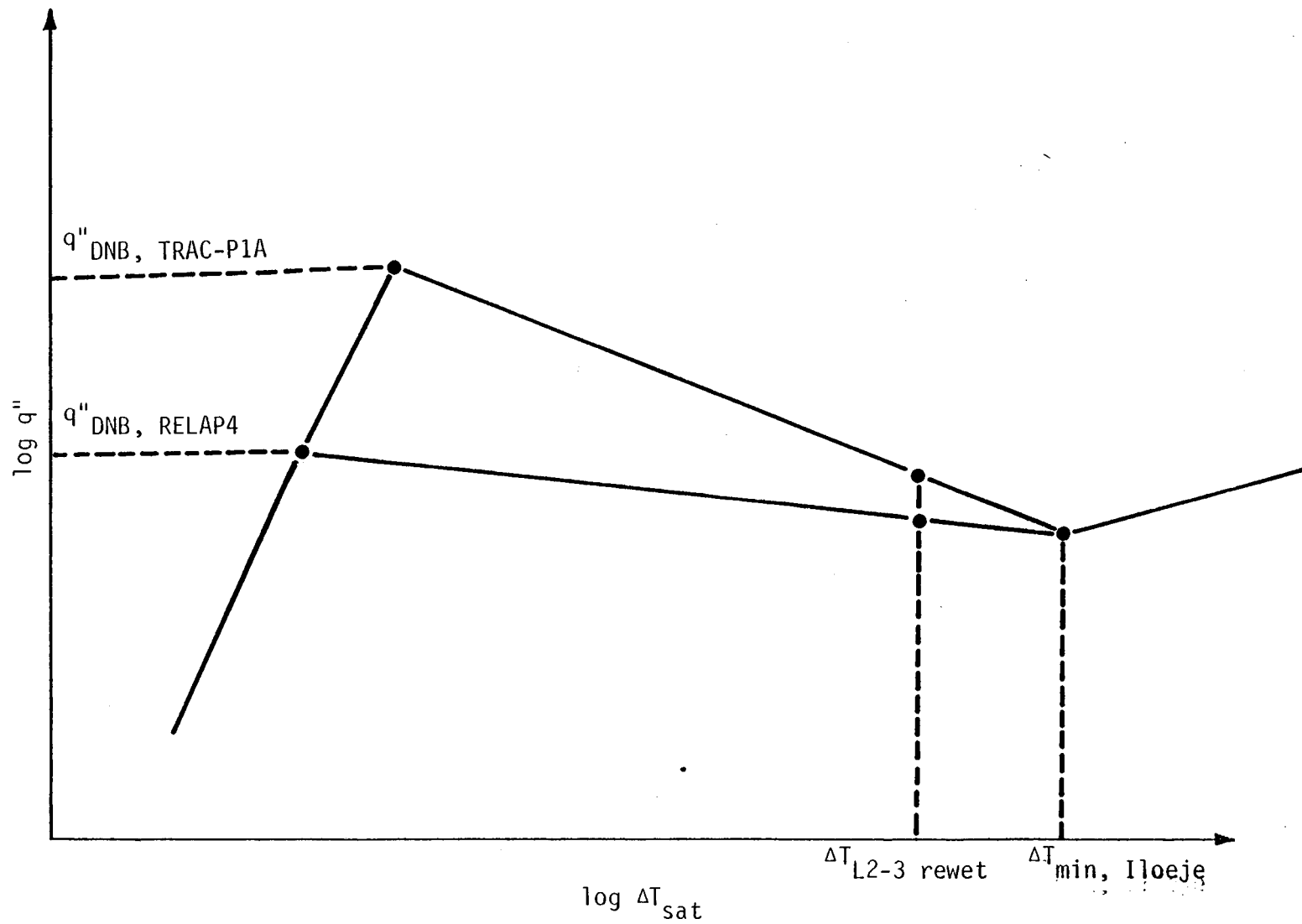


Figure 8. Effects of RELAP4 critical heat flux correlation on TRAC-P1A.

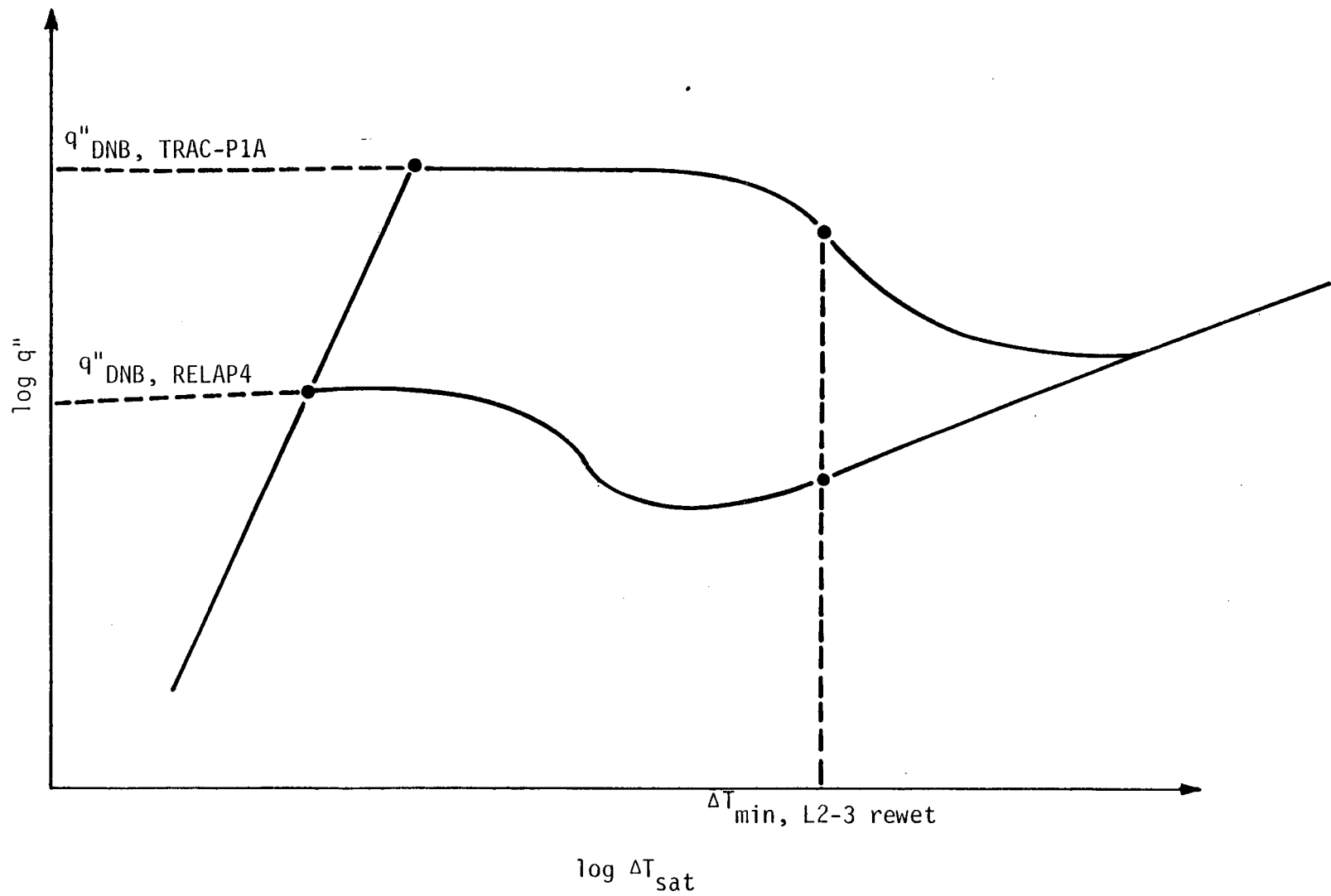


Figure 9. Effects of TRAC-P1A critical heat flux correlations on RELAP4/MOD6.

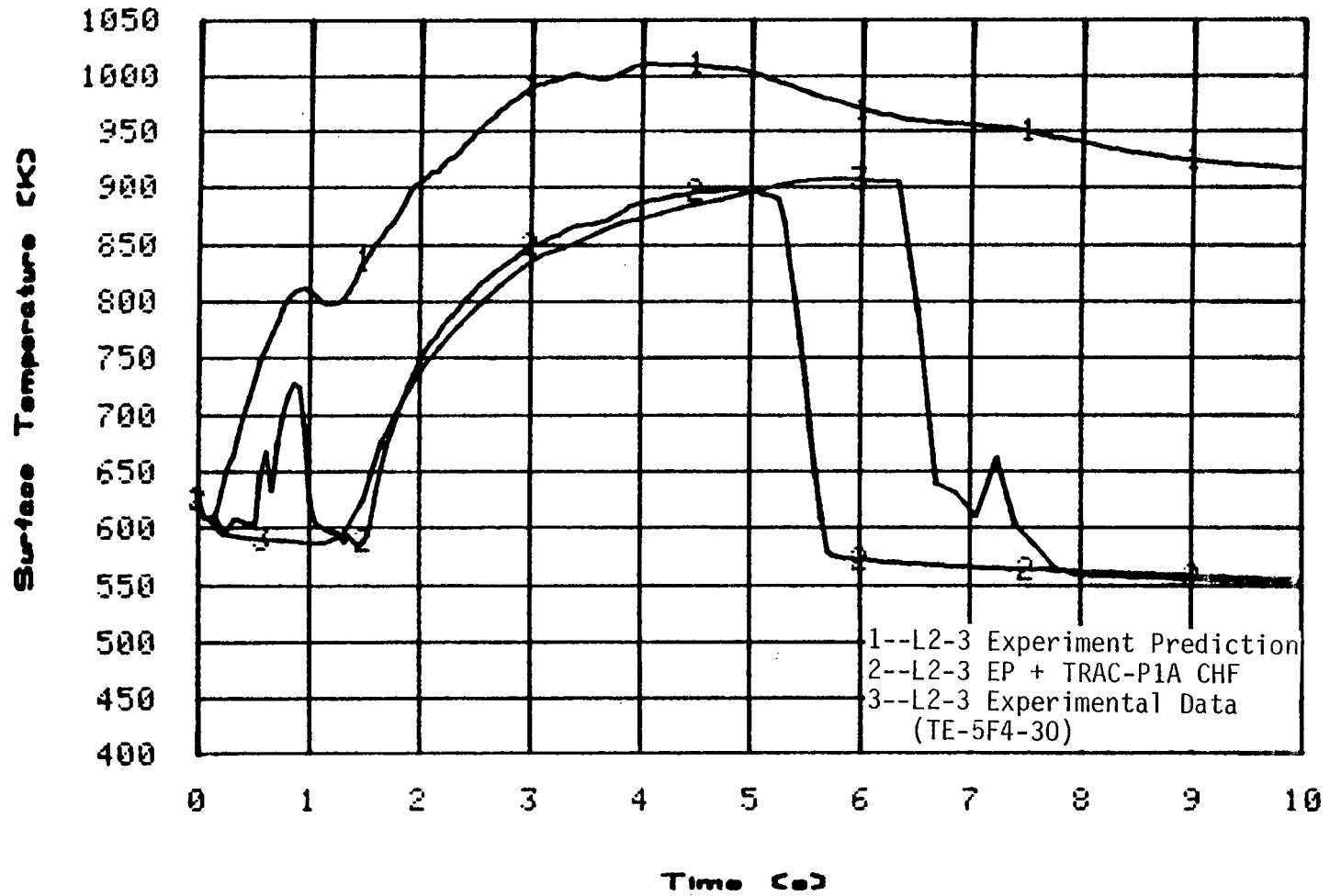


Figure 10. Effects of TRAC-P1A critical heat flux correlation on RELAP4/MOD6 calculated cladding temperature.

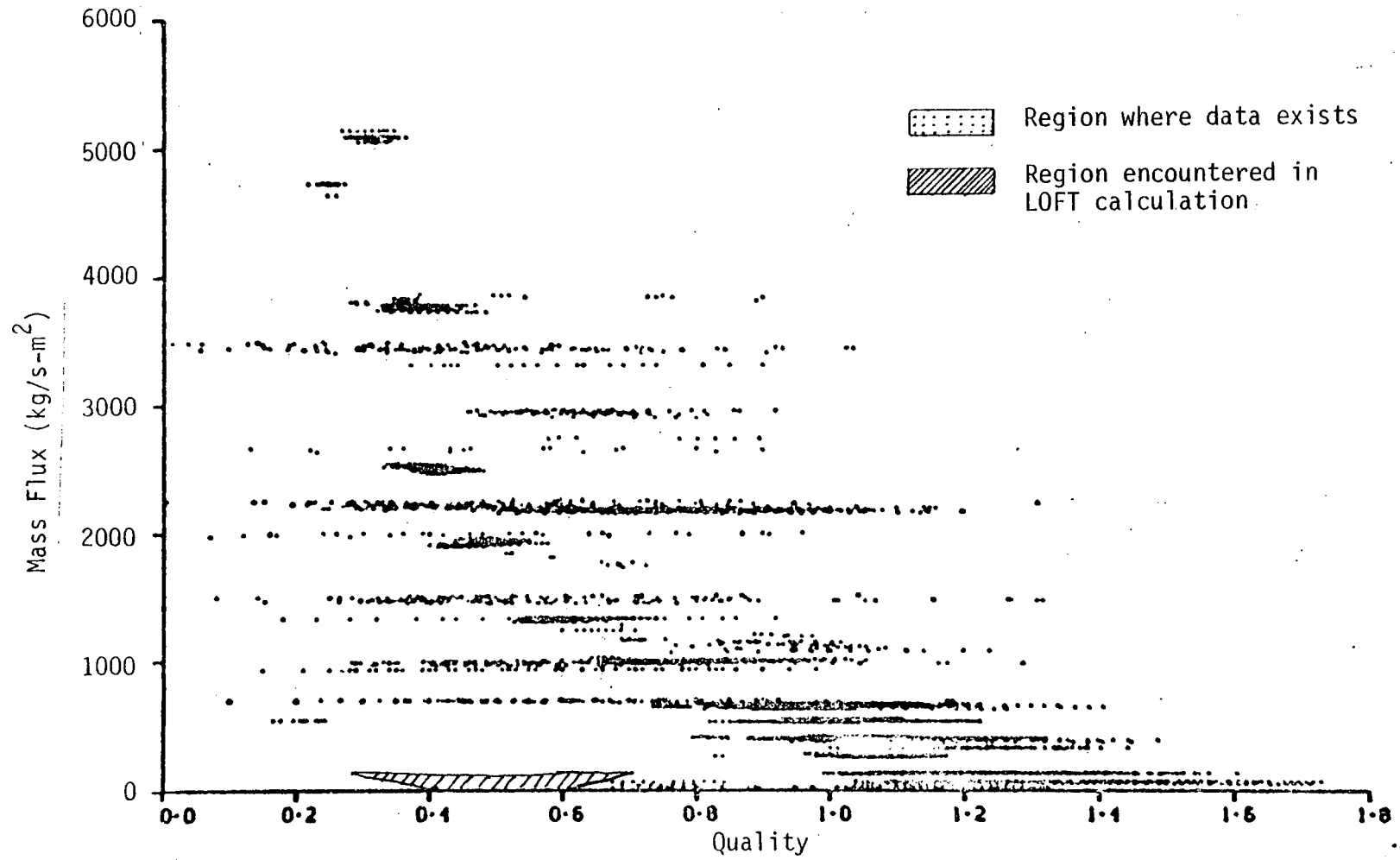


Figure 11. Comparison of fluid conditions in post-critical heat flux data base and LOFT calculations.

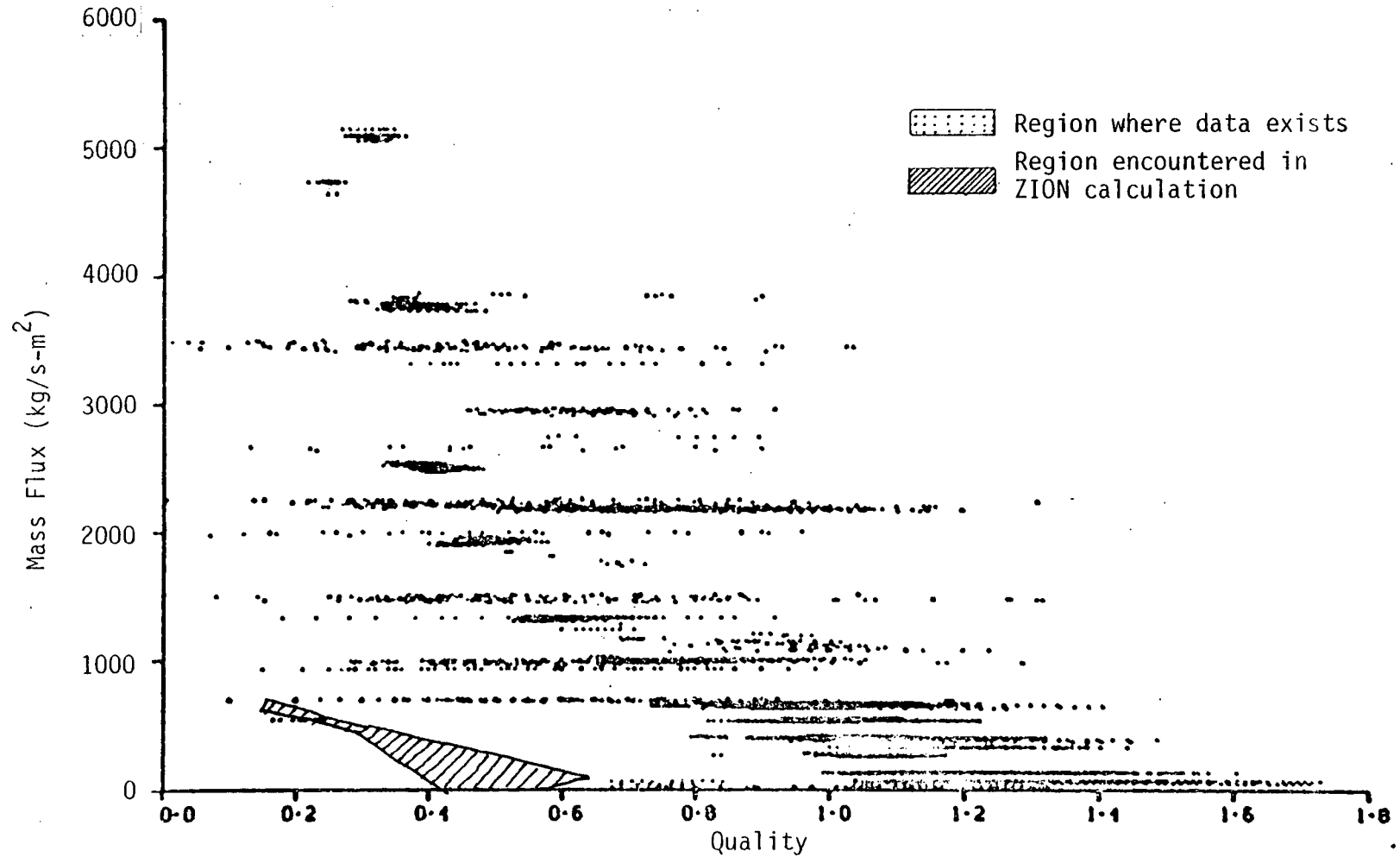


Figure 12. Comparison of fluid conditions in post-critical heat flux data base and ZION calculations.